

All optical switching and continuum generation in silicon waveguides

Özdal Boyraz, Prakash Koonath, Varun Raghunathan, and Bahram Jalali

Optoelectronic Circuits and Systems Laboratory
University of California, Los Angeles
Los Angeles, CA 90095
jalali@ucla.edu
<http://www.ee.ucla.edu/labs/oecs/>

Abstract: First demonstration of cross phase modulation based interferometric switch is presented in silicon on insulator waveguides. By using Mach-Zehnder interferometric configuration we experimentally demonstrate switching of CW signal ~25 nm away from the pump laser. We present the effect of free carrier accumulation on switching. Additionally, we theoretically analyze the transient effects and degradations due to free carrier absorption, free carrier refraction and two photon absorption effects. Results suggest that at low peak power levels the system is governed by Kerr nonlinearities. As the input power levels increase the free carrier effects becomes dominant. Effect of free carrier generation on continuum generation and power transfer also theoretically analyzed and spectral broadening factor for high input power levels is estimated.

©2004 Optical Society of America

OCIS codes: (190.4390) Nonlinear optics, integrated optics, (230.4320) Nonlinear optical devices, (230.7370) Waveguides, (250.5300) Photonic integrated circuits.

References and Links

1. R. Claps, D. Dimitropoulos, Y. Han, and B. Jalali, "Observation of Raman emission in silicon waveguides at 1.54 μm ," *Opt. Express* **10**, 1305-1313 (2002), <http://www.opticsexpress.org/abstract.cfm?URI=OPEX-10-22-1305>
2. J.J. Wayne, "Optical third-order mixing in GaAs, Ge, Si, and InAs," *Phys. Rev.* **178**, 1295-1303 (1969)
3. Peter Y. Yu, and Manuel Cardona, *Fundamentals of Semiconductors Physics and Materials Properties*, (Springer, 2001)
4. A. Villeneuve, C.C. Yang, G.I. Stegeman, C.N. Ironside, G. Scelsi, R.M. Osgood; "Nonlinear Absorption in a GaAs Waveguide Just Above Half the Band Gap," *IEEE J. Quant. Electron.* **30** (5) 1172-1175 (1994).
5. A.M. Darwish, E.P. Ippen, H.Q. Lee, J.P. Donnelly, S.H. Groves; "Optimization of four-wave mixing conversion efficiency in the presence of nonlinear loss," *Appl. Phys. Lett.* **69** (6) 737-739 (1996).
6. Y.-H. Kao, T.J. Xia, M.N. Islam; "Limitations on ultrafast optical switching in a semiconductor laser amplifier operating at transparency current," *J. Appl. Phys.* **86** (9) 4740-4747 (1999).
7. R. A. Soref, and J. P. Lorenzo, "All-silicon active and passive guided wave components for $\lambda=1.3$ and $1.6\mu\text{m}$," *IEEE J. Quantum Electron.* **22**, 873-879 (1986)
8. A. Cutolo, M. Iodice, P. Spirito, and L. Zeni, "Silicon electro-optic modulator based on a three terminal device integrated in a low loss single mode SOI waveguide," *J. Lightwave Technol.* **15**, 505-518 (1997).
9. C. K. Tang and G. T. Reed, "Highly efficient optical phase modulator in SOI waveguides," *Electron. Lett.* **31**, 451-452, (1995)
10. C. Z. Zhao, G. Z. Li, E. K. Liu, Y. Gao, and X. D. Liu, "Silicon on insulator Mach-Zehnder waveguide interferometers operating at 1.3 μm ," *Appl. Phys. Lett.* **67**, 2448-2449 (1995).
11. G. V. Treyz, P. G. May, and J. M. Halbout, "Silicon Mach-Zehnder waveguide interferometers based on the plasma dispersion effect," *Appl. Phys. Lett.* **59**, 771-773 (1991)
12. R. Claps, D. Dimitropoulos, V. Raghunathan, Y. Han, B. Jalali, "Observation of stimulated Raman amplification in silicon waveguides," *Opt. Express* **11**, 1731-1739 (2003) , <http://www.opticsexpress.org/abstract.cfm?URI=OPEX-11-15-1731>

13. R. Claps, V. Raghunathan, D. Dimitropoulos, B. Jalali, "Anti-Stokes Raman conversion in Silicon waveguides," *Opt. Express* **11**, 2862-2872 (2003),
<http://www.opticsexpress.org/abstract.cfm?URI=OPEX-11-22-2862>
 14. D. Dimitropoulos, V. Raghunathan, R. Claps, B. Jalali, "Phase-matching and nonlinear optical process in silicon waveguides," *Opt. Express* **12**, 149-160 (2004),
<http://www.opticsexpress.org/abstract.cfm?URI=OPEX-12-1-149>
 15. D. Dimitropoulos, V. Raghunathan, R. Claps, B. Jalali, "Phase matching and nonlinear optical process in silicon waveguides," *Proceedings of IPR 2004*, Paper IThE3, (2004)
 16. J. I. Dadap, R. L. Espinola, R. M. Osgood, Jr., S. J. McNab, Y. A. Vlasov, "Spontaneous Raman scattering in a silicon wire waveguide," *Proceedings of IPR 2004*, Paper IWA4, (2004)
 17. T.K. Liang, H.K. Tsang, I.E. Day, J. Drake, A.P. Knights, and M. Asghari, "Silicon waveguide two-photon absorption detector at 1.5 μ m wavelength for autocorrelation measurements," *Appl. Phys. Lett.* **81**, 1323-1325 (2002).
 18. T.K. Liang, H.K. Tsang; "Role of free carriers from two-photon absorption in Raman amplification in silicon-on-insulator waveguides," *Appl. Phys. Lett.* **84** (15) 2745-2747 (2004).
 19. R. Claps, V. Raghunathan, D. Dimitropoulos, and B. Jalali "influence of nonlinear absorption on Raman amplification in Silicon waveguides," *Opt. Express* **12**, 2774-2780 (2004),
<http://www.opticsexpress.org/abstract.cfm?URI=OPEX-12-12-2774>
 20. A. R. Cowan, G. W. Rieger, and J. F. Young, "Nonlinear transmission of 1.5 μ m pulses through single-mode silicon-on-insulator waveguide structures," *Opt. Express* **12**, 1611-1621 (2004),
<http://www.opticsexpress.org/abstract.cfm?URI=OPEX-12-8-1611>
 21. M. Dinu, F. Quochi, and H. Garcia, "Third-order nonlinearities in silicon at telecom waveguides," *Appl. Phys. Lett.* **82**, 2954-2956 (2003)
 22. H. K. Tsang, C. S. Wong, T. K. Liang, I. E. Day, S. W. Roberts, A. Harpin, J. Drake, and M. Asghari, "Optical dispersion, two-photon absorption and self-phase modulation in silicon waveguides at 1.5 μ m wavelength," *Appl. Phys. Lett.* **80**, 416-418 (2002)
 23. O. Boyraz, T. Indukuri, and B. Jalali, "Self-phase-modulation induced spectral broadening in silicon waveguides," *Opt. Express* **12**, 829-834 (2004),
<http://www.opticsexpress.org/abstract.cfm?URI=OPEX-12-5-829>
 24. Freeouf, J.L., Liu, S.T. *Proceedings of IEEE International SOI Conference. Tucson, AZ*, 74-75 (1995).
 25. Mendicino, M.A. Comparison of properties of available SOI materials. *Properties of Crystalline Silicon*. Ed. Hull, Robert. *INSPEC, IEE*. 992-1001 (1998).
 26. Kuwuyama, T., Ishimura, M., Arai, E. Interface recombination velocity of Silicon-on-insulator wafers measured by microwave reflectance photoconductivity method with electric field. *Appl. Phys. Lett.* **83**, 928-930 (2003).
 27. K. W. DeLong, A. Gabel, C. T. Seaton, and G. I. Stegeman, "Nonlinear transmission, degenerate four-wave mixing, photodarkening, and the effects of carrier-density-dependent nonlinearities in semiconductor-doped glasses," *Journal of Opt. Soc. Am. B* **6**, 1306-1313 (1989)
 28. R. A. Soref, and B. R. Bennett, "Electrooptical effects in silicon," *IEEE J. Quantum Electron.* **23**, 123-129 (1987)
 29. G. P. Agrawal, *Nonlinear Fiber Optics*, (Academic Press, 1995)
-

1. Introduction

The third-order nonlinear optical effects in silicon are much stronger than those in the optical fiber. Among the third order effects (i) Raman (ii) Kerr Nonlinearity (iii) Two Photon Absorption (TPA) are particularly strong. Compared to the optical fiber, Raman effect is 10^4 times stronger in silicon while the Kerr effect is 10^2 times stronger than that of the fiber [1,2]. Although, Raman effect is nearly 2 orders of magnitude stronger than the Kerr nonlinearity, under pulsed operation the Raman effect is suppressed as long as the pulse width is less than the phonon de-phasing time (~ 10 ps) [3]. Additionally, the high index contrast in Silicon On Insulator (SOI) waveguides results in tight mode confinement and improves the effective nonlinearity. In principle, it is thus possible to exploit the Kerr effect to perform optical switching. Unfortunately, TPA and TPA-induced Free Carrier Absorption (FCA) are also prominent in semiconductor waveguides. These phenomena have been identified as problematic in achieving efficient nonlinear optical devices in III-V compound

semiconductors [4-6] and must be dealt with in design of silicon based nonlinear optical devices.

Research on optical properties of silicon spans approximately three decades [2]. Absorption and refraction modulation through Free Carrier (FC) injection has been the subject for much of the research [7-11]. Recently, attention has focused on Raman effects in silicon. Optical amplification using Stimulated Raman Scattering (SRS) and Raman-induced wavelength conversion have been demonstrated in silicon waveguides [12-16]. Additionally, Two Photon Absorption (TPA) has been investigated as a means to create an Si autocorrelator device [17]. TPA-induced FCA has been studied in the potential limit to achievable Raman efficiency [18-19] and in transmission of ultra short pulses in silicon waveguides [20]. With respect to the Kerr nonlinearity in silicon, measurements of $\chi^{(3)}$ have been reported for bulk samples [2,21] and waveguides [22] with results suggesting a value that is two orders of magnitude higher than that in silica glass. Recently, we have demonstrated spectral broadening as a first step towards on-chip supercontinuum generation [23]. This was achieved through Self Phase Modulation (SPM) and at moderate peak power levels where FC effects were negligible. Specifically, a phase shift of approximately 2π was measured at the optical intensity of 2 GW/cm^2 .

In this paper, we demonstrate interferometric all-optical switching through Cross Phase Modulation (XPM) in silicon waveguides. To the best of our knowledge, this is the first such report. By using the Mach-Zehnder configuration, we experimentally demonstrate switching of CW signal in a $2\mu\text{m}^2$ silicon waveguide. A $\sim 7 \text{ ns}$ switching window, limited by FC accumulation, is observed. Additionally, we model optical switching and continuum generation in silicon waveguides including TPA-induced FC loss and index change. Results suggest that at low peak power levels the devices are governed by Kerr nonlinearities and switching can be obtained at approximately 40W pulse peak power levels with ultra fast response. As peak power level increases, free-carrier effects become important. Such effects include distortion in the switching transient and an enhancement of continuum generation with an asymmetric spectral profile.

2. Experimental results

The experimental setup used for XPM based interferometric switching in silicon is shown in Fig. 1. A modelocked fiber laser operating at 1560 nm with 20 MHz repetition rate is used to create $< 1\text{ps}$ pulses. Such short pulses are desirable in order to suppress the Raman interaction. The probe signal is generated by a CW laser at 1537 nm. After amplification, the pump and the probe are combined by a 10/90 coupler before entering a polarization beam splitter (PBS). The polarizations of the pump and signal are adjusted such that while the pump is directed to the silicon waveguide, the signal beam is split between the waveguide and the upper path of the interferometer. A tunable retro-reflector is inserted in the upper path of the interferometer to adjust the relative delay between two paths. The beams from the two paths are combined by

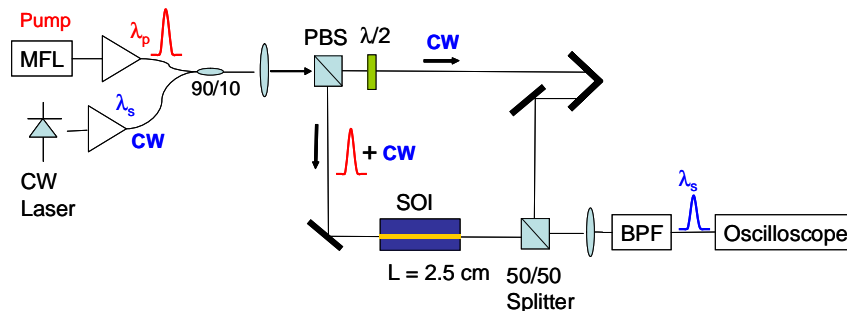


Fig. 1. Experimental setup of XPM based silicon switch. Mach Zehnder interferometer is used for switching. XPM induced phase shift causes switching of CW signal to the output port.

a 50/50 splitter. The pump is removed from the interferometer output using a bandpass filter. The switched signal is recorded by a realtime digitizing oscilloscope with a 4 GHz analog input bandwidth and 20 Gsample/s sampling rate after detecting by an external 20GHz photodetector. The silicon waveguide resides in the lower path of the interferometer and, is 2.5cm long with $2\mu\text{m}^2$ effective modal area. The input pump power to the silicon waveguide is measured to be ~ 15 mW. The average CW probe power is set to ~ 10 mW at the input of the waveguide. The output power collected in the fiber patchcord is measured to be $50 \mu\text{W}$. The total insertion loss of the waveguide is measured to be 13 dB, which includes coupling and propagation losses.

Figure 2 shows the experimental results of the XPM based interferometric switch. The relative delay between the arms is set such that in the absence of the pump, the probe beam suffers destructive interference and hence does not appear at the output. As shown in Fig. 2(a) a small amount of pump leakage is present when the signal laser is turned off. This is due to the broadening of the pump spectrum in the fiber patch cord preceding the interferometer. Figure 2(b) shows the net switching signal obtained by subtracting the residual pump signal from the measure signal. As can be seen, the signal beam is clearly switched on with 13 dB on-off ratio when the pump pulse is present. This is caused by the pump induced phase shift in the silicon waveguide resulting in constructive interference in the Mach Zehnder output. The phase shift has contributions due to XPM and due to the index change caused by TPA generated free carriers. Consequently, the switching transient is composed of a fast response with a width that is limited by the oscilloscope bandwidth, followed by an exponential decay with ~ 7 ns characteristic time constant. The fast response is due to XPM while the exponential decay has the characteristics of the FC effect. As will be shown in the next section, this behavior is consistent with a physical model that includes these phenomena. The measurements also suggest that the effective FC lifetime in the waveguide is ~ 7 ns.

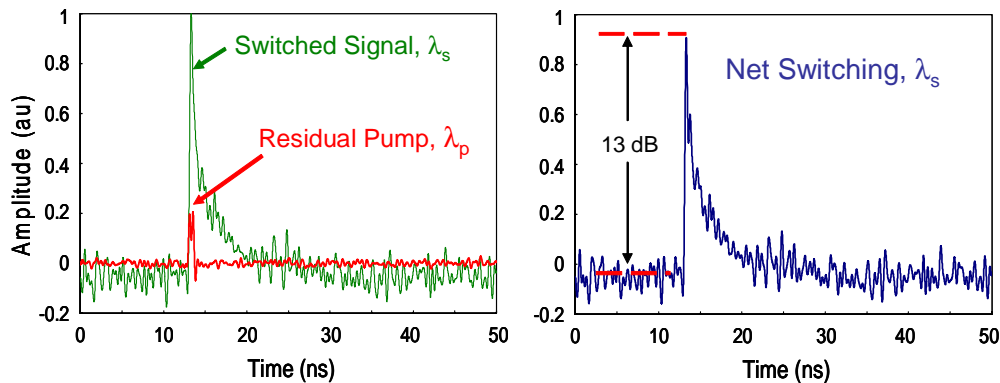


Fig. 2. Output results of XPM based silicon switch. a) Residual pump pulse and switched CW signal when probe signal is present. b) Net switching results. Exponential decay indicates free carrier refraction.

Figure 2 indicates that the switching transients are limited by the FC lifetime. The carrier lifetime in silicon-on-insulator samples depends on the method used for fabrication of the wafer and the film thickness, with reported values ranging between 10–200ns [18,19,24-25]. The lifetime is primarily limited by recombination caused by defect states located at the interface between the silicon and buried oxide. In rib waveguides, the lifetime is further reduced by lateral diffusion of carriers away from the optically active waveguide core. The effective lifetime of carriers in SOI waveguides can be written as: $1/\tau_{\text{eff}} = 1/\tau_r + 1/\tau_{\text{tr}}$, which includes the recombination lifetime τ_r and the transit (or diffusion) time τ_{tr} . Since carriers must diffuse to the interface for recombination to take place, τ_r is linearly proportional to Si film thickness [26]. Similarly, the transit time, τ_{tr} is proportional to rib width. Hence reducing

the waveguide cross section is beneficial as it reduces the effective lifetime and thus minimizes TPA-induced FCA.

3. Theoretical results

The relevant effects that need to be considered in the theoretical model are (i) Kerr nonlinearity and (ii) TPA induced pump depletion, (iii) absorption by TPA generated free carriers, and (iv) dispersion. Dispersion can be ignored in this case because of the fact that nonlinear length is much shorter than the dispersive length in these waveguides [23]. The following set of coupled equations then govern the pulse propagation in a nonlinear semiconductor waveguide [27-29,7]:

$$\frac{\partial E(t, z)}{\partial z} = -\frac{1}{2}(\alpha + \Delta\alpha + \alpha_{TPA})E(t, z) - ig\gamma |E_p(t, z)|^2 E + i\frac{2\pi}{\lambda} \Delta n E(t, z) \quad (1)$$

$$\Delta\alpha = \frac{e^3 \lambda^2}{4\pi^2 c^3 \epsilon_0 n} \left[\frac{\Delta N_e}{m_{ce} \cdot \mu_e} + \frac{\Delta N_h}{m_{ch} \cdot \mu_h} \right] \quad (2)$$

$$\Delta n = -\frac{e^2 \lambda^2}{8\pi^2 c^2 \epsilon_0 n} \left[\frac{\Delta N_e}{m_{ce}} + \frac{\Delta N_h}{m_{ch}} \right] \quad (3)$$

$$\frac{\partial N(t, z)}{\partial t} = -\frac{N(t, z)}{\tau_{eff}} + \beta \frac{I_p(t)^2}{2\hbar\omega} \quad (4)$$

$$\alpha_{TPA} = \frac{4n}{480\pi A_{eff}^2} \beta I_p(t, z) \quad (5)$$

Equation (1) is a modified version of the Non-Linear Schrödinger Equation (NLSE) without dispersive effects [29]. The parameter E describes the signal envelope. The first term on the RHS describes the waveguide propagation loss, FCA and TPA. The second term describes the nonlinear phase shift. The parameter g is a constant which is equal to 2 for the XPM and is unity for SPM. E represents the signal field in XPM and the pump field in SPM. The parameter γ is the nonlinearity constant given in reference [23] and has a value of 1000 (1/W.m) in our waveguide with $A_{eff} = 5\mu\text{m}^2$ modal area. The last term gives the phase accumulation due to FC refraction. The Eqs. (2) and (3) describe the changes in the refractive index, n , and absorption, α , caused by free carriers [28]. N_e and N_h are the generated electron and hole concentrations respectively, λ is the wavelength, m is the effective mass and μ is the mobility. Equation (4) describes FC recombination and generation. The parameter N represents FC density, τ_{eff} is the FC lifetime, β is the TPA coefficient [23] I_p is the intensity of the pump signal, and E_p is the photon energy. The last equation describes the pump attenuation due to TPA.

3.1 Optical switching

We first consider the nonlinear phase shift in the waveguide. The phase shift has two sources, (i) the Kerr nonlinearity, and (ii) the FC induced index change. Free carriers are generated by the optical pulse and decay during the interval between pulses. Hence, their transient behavior (which determines the index change) and their average density (which determines the absorption) depend on the ratio of the pulse repetition period, T , and the effective recombination lifetime, τ_{eff} . Figure 4(a) shows the contribution of FC induced index change to the nonlinear phase shift. The behavior is highly sensitive to the ratio of T/τ_{eff} . For $\tau_{eff} \ll 1$, the carrier accumulation results in a significantly higher phase shift compared to that caused by Kerr effect. However, this is not useful for fast switching applications since it is the steady

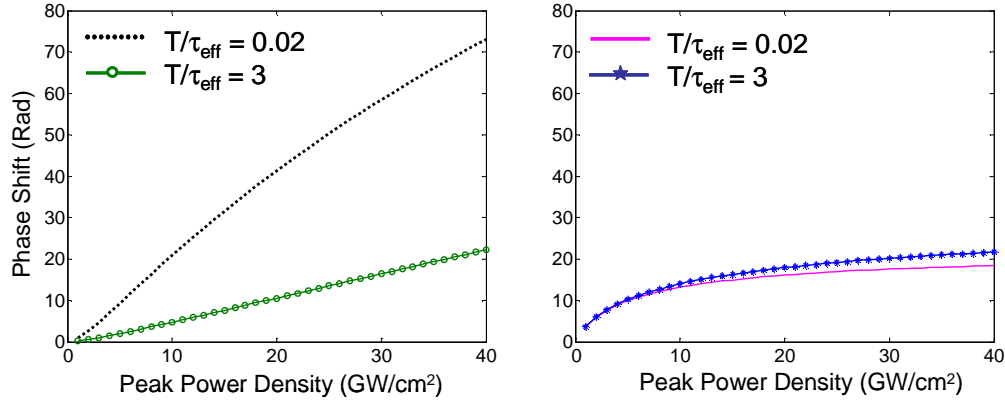


Fig. 4. Total amount of phase shift for two different free carrier lifetime values induced by a) the index change due to free carrier accumulation and b) the Kerr nonlinearity. T = pulse period and τ_{eff} = free carrier life time.

state value caused by buildup in carrier density. The detailed switching behavior that will result from this phenomenon is shown in Fig. 6(b) and will be discussed below. Figure 4(b) shows the contributions of the Kerr effect to the nonlinear phase shift. Calculations are done for two different T/τ_{eff} values to show the impact of FC loss. The observed saturation is due to the pump depletion caused by TPA. For $T/\tau_{\text{eff}} \ll 1$, FC accumulation occurs resulting in higher losses and a slightly lower phase shift.

Figure 5 shows the comparison of the Kerr and the FC contributions for the ideal case when the lifetime is shorter than the pulse period ($\tau_{\text{eff}}=3$). As can be seen a 180° phase shift can be achieved at relatively low peak power of $\sim 100\text{W}$ and in this regime, Kerr nonlinearity dominates the FC effect. This is the regime of interest for optical switching and it requires the lifetime to be shorter than the pulse repetition period. Typical values for the minority carrier lifetime in silicon waveguides is discussed in Section 4.

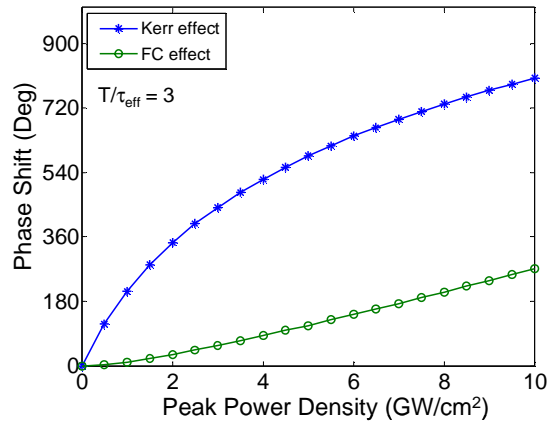


Fig. 5. Total amount of phase shift induced by the index change due to free carrier accumulation and the Kerr nonlinearity in the absence of free carrier accumulation. 180° phase shift can be obtained by Kerr nonlinearity at moderate power levels and with minimal free carrier effect.

Figure 6(a) shows the switching behavior for two different peak power levels. Simulations are performed for $T/\tau_{\text{eff}}=3$ and with $\tau_{\text{eff}}=1$ ns. At 40W Kerr nonlinearity dominates whereas at 2000W , FC effect is the main source of nonlinear phase shift. At 2000W power levels, the switching transient exhibits an exponential decay with a time constant that is consistent with the carrier lifetime. Figure 6(b) shows the detailed transient behavior over the time scale of the pump pulse. For the low pump power where the Kerr

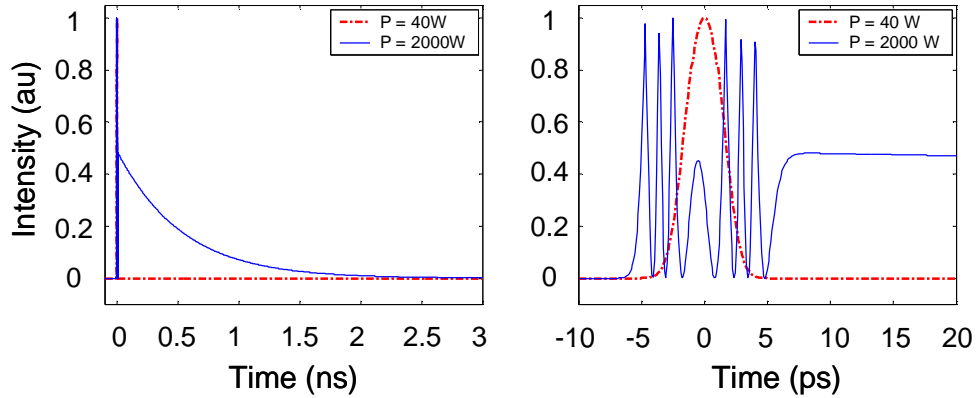


Fig. 6. Simulated switching behavior in silicon. a) full scale representation b) 30ps time window of switched signal. Perfect switching profile is obtained at 40W peak power levels.

effect dominates, the output signal pulse closely follows the shape of the pump pulse (FWHM=4ps). At the 2000W peak power levels, the switched signal initially has an oscillatory behavior. This is expected because the total phase shift is much greater than 180° , Fig. 4(b). The simulation results and the experimental data shown earlier are encouraging as they indicate that all-optical switching can be realized in silicon waveguide with moderate peak powers.

3.2 Continuum generation

Previously, we have experimentally demonstrated spectral broadening in silicon waveguides [23]. The range of power levels encountered in the experiment was low enough such that FC effects did not need to be included in the theoretical model. Here, we consider a general case and use the model developed in the previous section to study the impact of TPA generated free carriers on spectral broadening in silicon waveguides. The simulations are conducted for three different conditions: (i) without FC effect, (ii) for $T/\tau_{\text{eff}} > 1$ where generated carriers recombine within the inter-pulse period, and (iii) for $T/\tau_{\text{eff}} \ll 1$ where significant carrier accumulation takes place.

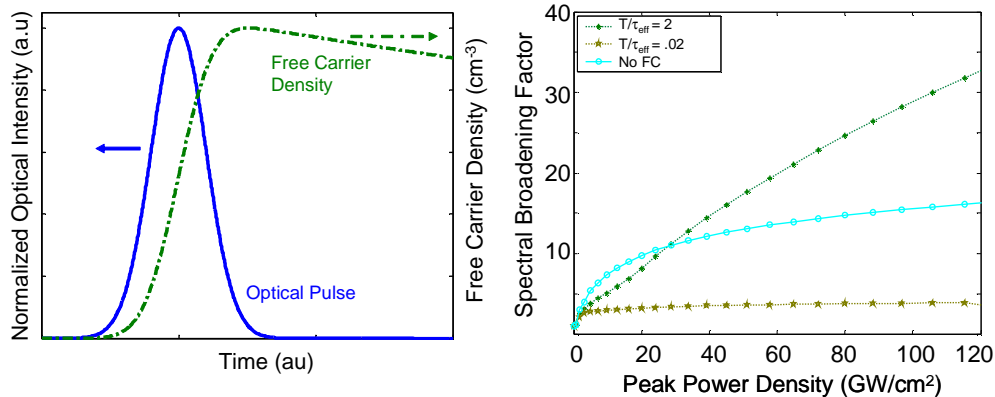


Fig. 7. a) Qualitative depiction of free carrier transients in the time scale of optical pulse. The free carrier density follows the integral of pulse shape. b) Simulated results of spectral broadening factor.

Figure 7(a) is a qualitative depiction of the FC transient on the time scale of an optical pulse. In general, the FC density follows the integral of the pulse shape. Since the FC induced phase shift is proportional to the carrier density, the trailing edge of the pulse sees a higher phase shift than the leading edge. This give rise to an asymmetric spectral broadening, which

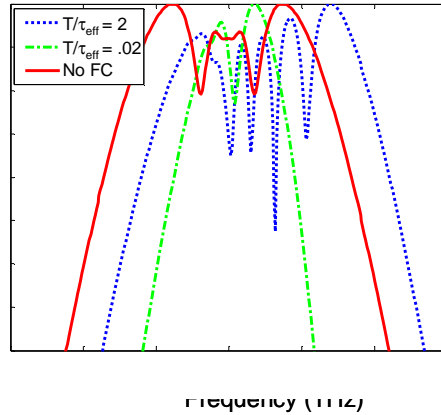


Fig. 8. Spectrum generated at ~ 25 GW/cm². SPM generates symmetric spectral broadening and free carrier refraction generate blue shifted spectrum.

was not observed in our previous experiments due to limited power levels but has been observed in later experiments performed by Cowan *et al.* [20]. Figure 7(b) plots the calculated spectral broadening factor as a function of peak pulse intensity. To assess the impact of the FC transient, simulation are performed for cases of $T/\tau_{\text{eff}} = 2$ and $T/\tau_{\text{eff}} = 0.02$. We observe that significantly higher broadening for the first case where carriers do not accumulate and hence FCA is negligible. To determine the relative contributions to spectral broadening of FC effect vs. Kerr effect, we also plot the broadening factor in the absence of FC effect. In the absence of the FC effect, pump depletion due to TPA limits the spectral broadening at high pump intensities. The FC induced index has opposite sign compared to the index change induced by the Kerr effect. Therefore, FC effect tends to reduce the spectral broadening until at high intensities (>30 GW/cm²) where it dominates and provides a larger spectral broadening factor.

Figure 8 shows the simulated spectrum at 25 GW/cm². In the absence of FC effects, a symmetric spectrum is observed. Since the FC accumulation follows the integral of the pulse shape, the trailing edge of the pulse sees a higher phase shift than the leading edge, leading to an asymmetrical spectrum. In particular the spectrum is blue shifted. In the presence of FC accumulation, low spectral broadening with small asymmetry is obtained, Fig. 7(b). These observations are consistent with those reported in [20].

Previously Cowan *et al.* [20] have reported observation of negative differential transmission for silicon waveguides beyond a certain power level, however, the observation

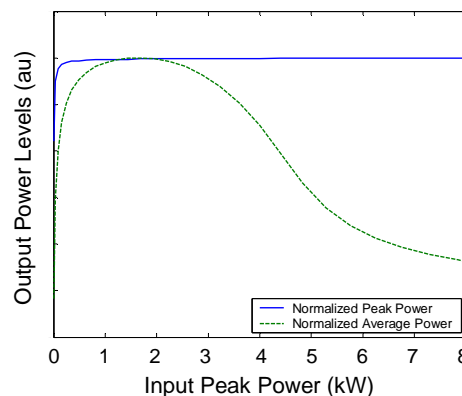


Fig. 9. Power transfer function in the presence of pulse steepening. Free carrier absorption causes higher attenuation at the trailing edge of the pulse and average throughput reduces. On the other hand peak power level shows saturated behavior due to TPA.

could not be accounted for in the simulations [20]. Using the above model, we can explain this observation by distinguishing between peak and average powers. Similar to the index change, the FCA also follows the integral of the pulse shape. Thus the trailing edge of the pulse is more attenuated than the leading edge. This causes pulse steepening at extremely high power levels. Figure 9 shows the peak and average power levels emerging from the waveguide. Model parameters are described in the caption. To facilitate the comparison, the values are normalized so they match at the maximum. The average power indeed shows a negative differential transmission due to pulse steepening. On the other hand, the peak power simply saturates. Since a power meter, used in [20] measures the average power, the measurements would exhibit a negative differential transmission [20]. However, this interesting phenomenon will not occur in real-time where it is most useful.

4. Summary

The above analysis suggests that all-optical switching in silicon will be governed by three processes: (i) Kerr effect, (ii) pump depletion due to TPA, and (iii) refraction and absorption due to free carriers generated by TPA. Free carriers impact both the switching time and the switching efficiency. For fast switching, the recombination lifetime must be similar or shorter than the pulse width. This is difficult to achieve in practice since high pulse peak powers that are needed to effect switching are typically achieved by using picosecond pulses. While the effective lifetime in submicron silicon waveguides (~ 1 ns) is much shorter than in bulk silicon ($\sim 1-10$ μ s) it is much longer than the optical pulse width. To avoid FCA and to obtain efficient switching, carrier accumulation must be avoided. This requires the lifetime to be much shorter than the pulse period, placing an upper limit on the repetition rate at which efficient switching can be achieved. Hence there is a direct trade-off between the data rate that can be switched and the required pump power. Fortunately, there exists a regime where the optical intensity is low enough such that the FC generation is negligible yet the Kerr induced phase shift of 180° can be achieved. As shown in Figure 5, this regime corresponds to peak intensity levels of ~ 1 GW/cm² or lower.

At high intensities (> 30 GW/cm²) the index change caused by FC generation is much larger than the Kerr induced index change, resulting in significant spectrum broadening. As long as the lifetime is much shorter than the repletion period, carrier accumulation and the resulting absorption is avoided. Therefore, the FC effect can be beneficial in supercontinuum generation at low repetition rates (< 1 GHz). However, a tradeoff exists between efficiency and repetition rate, similar to that in optical switching. In order to avoid FC accumulation at high repetition rate, the lifetime must be similar to or shorter than the pulse period, placing an upper limit on the repetition rate.